

Microwave Absorbing Properties of W-Type Hexaferrite $\text{Ba}(\text{MnZn})_x\text{Co}_{2(1-x)}\text{Fe}_{16}\text{O}_{27}$

Xianming Qin¹, Ying Cheng², Kesheng Zhou², Shengxiang Huang², Xia Hui^{2*}

¹Xiamen Hongye Project Build Technique Co. Ltd., Xiamen, China

²School of Physics and Electronics, Central South University, Changsha, China

Email: *xhui73@csu.edu.cn, 5430@csu.edu.cn

Received June 18, 2013; revised July 18, 2013; accepted August 25, 2013

Copyright © 2013 Xianming Qin *et al.* This is an open access article distributed under the Creative Commons Attribution License, which permits unrestricted use, distribution, and reproduction in any medium, provided the original work is properly cited.

ABSTRACT

MnZn-doped W-type barium cobalt ferrite powder composites of $\text{Ba}(\text{MnZn})_x\text{Co}_{2(1-x)}\text{Fe}_{16}\text{O}_{27}$ ($x = 0.1, 0.2, 0.3, 0.4,$ and 0.5) were prepared in a sol-gel process. The microwave absorbing properties of the composites in the range of 2 - 18 GHz and their electromagnetic loss mechanisms were studied. The results demonstrated that the synthesized $\text{Ba}(\text{MnZn})_x\text{Co}_{2(1-x)}\text{Fe}_{16}\text{O}_{27}$ samples possess a W-type phase of the crystal structure with a hexagonal flaky shape in micro-morphology, and the samples exhibited a soft magnetic trait that enables improving their microwave absorption properties through suitable MnZn doping. For $\text{Ba}(\text{MnZn})_{0.4}\text{Co}_{1.2}\text{Fe}_{16}\text{O}_{27}$ with a thickness of 2.8 mm, the reflection loss peak was -40.7 dB at a frequency of 7.3 GHz, with a bandwidth of 6.6 GHz at a loss of less than -10 dB. The microwave absorption primarily resulted from magnetic losses caused by magnetization relaxation, domain wall resonance, and natural resonance.

Keywords: Sol-Gel Process; W-Type Ferrite; Microwave Absorbing Materials; Electromagnetic Loss

1. Introduction

Ferrite is one type of the important electromagnetic-wave absorbing materials, of which spinel and magnetoplumbite hexagonal ferrites are the most widely used in applications. However, because of Snoek's limitation, the working frequency of those spinel ferrites is generally confined to the range below 3 GHz [1-5]. Hexagonal ferrites, which exhibit a planar anisotropy and ferromagnetic resonance in the GHz range caused by a high magneto-crystalline anisotropy field, are applicable for use as electromagnetic-wave absorption materials working in the GHz wavelength range [5-9]. Hexagonal ferrites can be classified into many types, including M-, Y-, W-, X-, Z-, and U-type phase, according to their chemical formulas and crystal structures. The M-type is the most studied among those hexagonal ferrites. It has been confirmed that different ions can be substituted for Ba^{2+} and Fe^{3+} in M-type phase ferrite, such as La for Ba^{2+} and Co-Ti, Mn-Ti, Mg-Ti, Co-Mn-Ti, Mn-Cu-Ti, Mn-Cu-Zr and Zn-Zr-Sn for Fe^{3+} . Consequently, the electromagnetic parameters of the ferrites can be adjusted or controlled, and their microwave absorption performance can be improved [2-7,10-17].

W-type phase ferrite can be viewed as a complex ferrite consisting of M-type phase and spinel phase block, which is $\text{M} + 2\text{S}$ (M: $\text{BaFe}_{12}\text{O}_{19}$, S: $\text{Fe}^{2+}\text{Fe}_2\text{O}_4$). In $\text{BaFe}_{12}\text{O}_{19}$, chemical doping is commonly utilized by replacing Fe^{2+} with Co^{2+} to improve its thermal stability and other properties, which results in a W-type barium-cobalt ferrite of $\text{BaCo}_2\text{Fe}_{16}\text{O}_{27}$. Because of the existing Fe^{2+} and Fe^{3+} cation sites, Fe cations are easily substituted by other divalent and trivalent cations; the magnetic parameters, including saturation magnetization, Curie temperature, coercivity, magnetic anisotropy and ferromagnetic resonance frequency, are thus more adjustable. However, there are fewer studies on microwave electromagnetic characteristics of W-type phase ferrites than on the characteristics of M-type ferrites. The substitution of Co^{2+} or Ba^{2+} by other metal ions was determined to help improve the microwave absorption properties of $\text{BaCo}_2\text{Fe}_{16}\text{O}_{27}$. Materials with improved microwave absorption include $\text{Ba}(\text{Zn}_x\text{Co}_{1-x})_2\text{Fe}_{16}\text{O}_{27}$ [10], $\text{BaZn}_{1.1}\text{Co}_{0.9}\text{Fe}_{16}\text{O}_{27}$ [13], $\text{Ba}_{1-x}\text{Er}_x(\text{Zn}_{0.3}\text{Co}_{0.7})_2\text{Fe}_{16}\text{O}_{27}$ [18] and $\text{Ba}(\text{Zn}_{0.5}\text{Co}_{0.5})_2\text{Fe}_{16}\text{O}_{27}$ [19]. The microwave electromagnetic effects are expected to be richer when Co^{2+} in $\text{BaCo}_2\text{Fe}_{16}\text{O}_{27}$ is substituted by two or more metal ions.

In this paper, MnZn-doped W-type barium cobalt fer-

*Corresponding author.

rite composites of $\text{Ba}(\text{MnZn})_x\text{Co}_{2(1-x)}\text{Fe}_{16}\text{O}_{27}$ were prepared using a sol-gel process. The microwave absorption properties of $\text{Ba}(\text{MnZn})_x\text{Co}_{2(1-x)}\text{Fe}_{16}\text{O}_{27}$ in the frequency range of 2 - 18 GHz are investigated, and the electromagnetic loss mechanism is discussed.

2. Experiments

2.1. Preparation of $\text{Ba}(\text{MnZn})_x\text{Co}_{2(1-x)}\text{Fe}_{16}\text{O}_{27}$ Powders

$\text{Ba}(\text{MnZn})_x\text{Co}_{2(1-x)}\text{Fe}_{16}\text{O}_{27}$ ($x = 0.1, 0.2, 0.3, 0.4$ and 0.5) were synthesized using a sol-gel process. According to the stoichiometric ratio of $\text{Ba}(\text{MnZn})_x\text{Co}_{2(1-x)}\text{Fe}_{16}\text{O}_{27}$, the weighed Fe^{3+} , Co^{2+} , Zn^{2+} , and Ba^{2+} nitrate and manganese acetate were dissolved in deionized water and stirred to form a uniform brown transparent solution. Citric acid was added to the above solution according to the molar ratio of 1:1.5 between the metal ions and the citric acid, and the ammonia water was dripped to ensure the pH value that was in the range of 6 - 7. Next, the solution was strung for 4 h in a water bath at 80°C to form a sol. The solution was then dried in an oven (100°C) to obtain the dry gels. The dry gels were slightly grinded after ashing at 450°C . Finally, the black $\text{Ba}(\text{MnZn})_x\text{Co}_{2(1-x)}\text{Fe}_{16}\text{O}_{27}$ ferrites were obtained by cooling the powder, which was sintered in an electric furnace at 1235°C for 4 h under the atmosphere circumstances.

2.2. Measurements

The crystal structure of $\text{Ba}(\text{MnZn})_x\text{Co}_{2(1-x)}\text{Fe}_{16}\text{O}_{27}$ ($x = 0.1, 0.2, 0.3, 0.4$ and 0.5) was investigated through X-ray diffraction (XRD) using a system from X'pert PRO of Holland PANalytical that utilized a Cu target at a voltage/current of 35-kV/25-mA. Scanning electron microscopy (SEM) examination was performed using QUANTA 200 to obtain the morphology and size of the powder particles of $\text{Ba}(\text{MnZn})_x\text{Co}_{2(1-x)}\text{Fe}_{16}\text{O}_{27}$. The hysteresis loops of the $\text{Ba}(\text{MnZn})_{0.4}\text{Co}_{1.2}\text{Fe}_{16}\text{O}_{27}$ particles were measured using a vibrating sample magnetometer (VSM).

The prepared crystalline powders were mixed with paraffin wax at a ratio of 8:3 in weight by heating and pressed into annular samples. The complex permittivity and permeability of the samples were measured using an AV3629 microwave vector network analyzer in the frequency range of 2 - 18 GHz. The relationship between microwave reflectivity (R) and frequency (f) can be obtained according to a previous formula [20,21] that used the measured data.

3. Results and Discussion

3.1. Crystal Structure, Morphology and Hysteresis Loop of the Powders

Figure 1 shows the XRD pattern of the

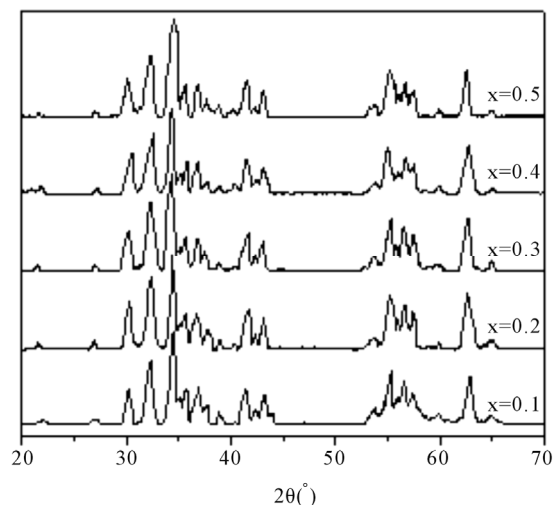


Figure 1. XRD pattern of $\text{Ba}(\text{MnZn})_x\text{Co}_{2(1-x)}\text{Fe}_{16}\text{O}_{27}$.

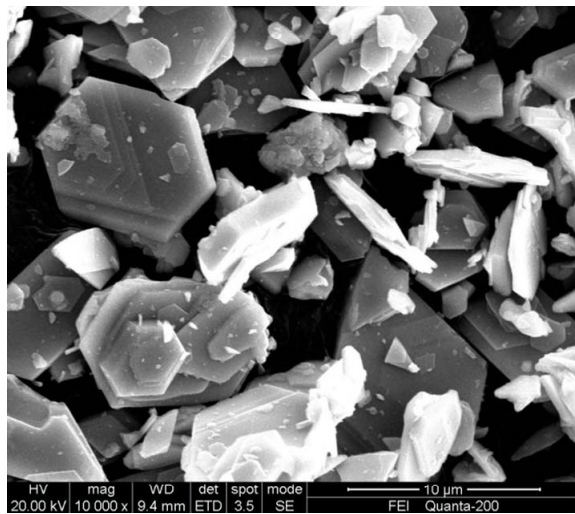
$\text{Ba}(\text{MnZn})_x\text{Co}_{2(1-x)}\text{Fe}_{16}\text{O}_{27}$ ($x = 0.1, 0.2, 0.3, 0.4$ and 0.5) ferrites calcined at 1235°C for 4 h. Compared with the characteristic diffraction peaks of the standard XRD card (PDF#19-0098) for W-type phase ferrite, the crystal structures of $\text{Ba}(\text{MnZn})_x\text{Co}_{2(1-x)}\text{Fe}_{16}\text{O}_{27}$ samples were measured to be a single W-type phase structure. Nearly no variations of the crystal structure were observed for all MnZn-doped $\text{Ba}(\text{MnZn})_x\text{Co}_{2(1-x)}\text{Fe}_{16}\text{O}_{27}$ samples when x was equal to 0.1, 0.2, 0.3, 0.4 and 0.5.

Figure 2 shows SEM images of $\text{Ba}(\text{MnZn})_{0.4}\text{Co}_{1.2}\text{Fe}_{16}\text{O}_{27}$ and $\text{Ba}(\text{MnZn})_{0.3}\text{Co}_{1.4}\text{Fe}_{16}\text{O}_{27}$ powders after high-temperature annealing at 1235°C for 4 h. The SEM images indicate that both the morphology of the $\text{Ba}(\text{MnZn})_{0.4}\text{Co}_{1.2}\text{Fe}_{16}\text{O}_{27}$ and $\text{Ba}(\text{MnZn})_{0.3}\text{Co}_{1.4}\text{Fe}_{16}\text{O}_{27}$ are hexagonal flaky with a clear outline. The average size was $5\ \mu\text{m}$ with a narrow distribution. As a result, doping with a small amount of MnZn does not significantly affect the grain size and morphology.

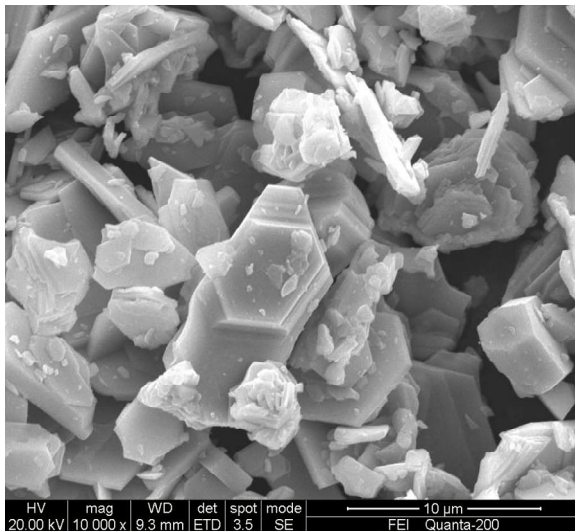
Figure 3 shows the hysteresis loop of $\text{Ba}(\text{MnZn})_{0.4}\text{Co}_{1.2}\text{Fe}_{16}\text{O}_{27}$ powders calcined at 1235°C for 4 h. The coercivity (H_c), magnetization (M_s) and retentivity (M_r) are 28.702 Oe, 67.320 emu/g, 3.7964 emu/g, respectively. The hysteresis loop indicates that $\text{Ba}(\text{MnZn})_{0.4}\text{Co}_{1.2}\text{Fe}_{16}\text{O}_{27}$ is a soft magnetic material.

3.2. The Microwave Absorption Properties

Figure 4 shows the variation of reflection loss versus frequency for $\text{Ba}(\text{MnZn})_x\text{Co}_{2(1-x)}\text{Fe}_{16}\text{O}_{27}$ ($x = 0.1, 0.2, 0.3, 0.4$ and 0.5) at a thickness of 2.8 mm. For $x = 0.1$, the reflection loss exhibits a peak at approximately -12 dB at a frequency of 8.1 GHz, with a bandwidth of 5 GHz for losses less than -10 dB. For $x = 0.2$, the reflection loss exhibits a peak at approximately -16 dB at 5.0 GHz, with a bandwidth of 6 GHz for losses less than -10 dB. For $x = 0.3$, the reflection loss exhibits a peak at ap-



(a)



(b)

Figure 2. SEM images of powders (a) $\text{Ba}(\text{MnZn})_{0.4}\text{Co}_{1.2}\text{Fe}_{16}\text{O}_{27}$ and (b) $\text{Ba}(\text{MnZn})_{0.3}\text{Co}_{1.4}\text{Fe}_{16}\text{O}_{27}$.

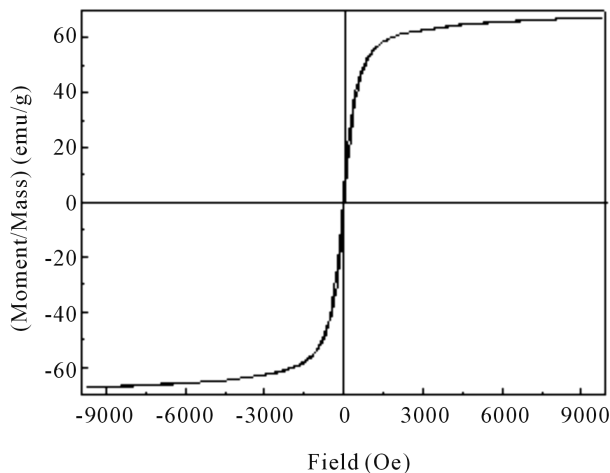


Figure 3. Hysteresis loop of $\text{Ba}(\text{MnZn})_{0.4}\text{Co}_{1.2}\text{Fe}_{16}\text{O}_{27}$.

proximately -23 dB at 8.0 GHz, with a bandwidth of 6.5 GHz for losses less than -10 dB. For $x = 0.4$, the reflection loss exhibits a peak at approximately -40.7 dB at 7.3 GHz, with a bandwidth of 6.6 GHz for losses less than -10 dB. For $x = 0.5$, the reflection loss exhibits a peak at approximately -12 dB at 5.5 GHz, with a bandwidth of 3 GHz for losses less than -10 dB. It was shown that the compositions $\text{Ba}(\text{MnZn})_{0.3}\text{Co}_{1.4}\text{Fe}_{16}\text{O}_{27}$ and $\text{Ba}(\text{MnZn})_{0.4}\text{Co}_{1.2}\text{Fe}_{16}\text{O}_{27}$ have obviously higher microwave absorptions than the other compositions. This would be explained by doped MnZn elements can change the electric and magnetic structures of the system, result in the change of the magnetocrystalline anisotropy field, the increase of the domain rotation resistance, pinning of domain wall displacement, thereby the magnetic loss is increased and the resonance frequency is changed. However, overdoping will increase the lattice distortion, result in the increase of electric resistivity and the decrease of Ohmic loss. Thus, the appropriate doping can enhance the impedance matching and microwave attenuation and change the position of the absorption peak. As a result, W-type barium-cobalt ferrite doped by certain amounts of MnZn can act as a wide-band microwave absorber. As shown in **Figure 4**, the frequency position of the absorption peak changes with the amount of doped MnZn. This absorption peak shifts with doping because the amount of doped material will affect the magnetocrystalline anisotropic field and thus cause a change in the natural resonance frequency.

Figure 5 shows the variation of the reflection loss versus frequency for $\text{Ba}(\text{MnZn})_{0.4}\text{Co}_{1.2}\text{Fe}_{16}\text{O}_{27}$ at different thicknesses. For $d = 2.0$ mm, the maximum reflection loss is approximately -17 dB at a frequency of 4.8 GHz, with a bandwidth of 3 GHz for losses less than -10 dB. For $d = 2.4$ mm, the maximum reflection loss is approximately -22.5 dB at a frequency of 5.5 GHz, with a bandwidth of 5 GHz for losses less than -10 dB. For $d = 2.8$ mm, the maximum reflection loss is approximately

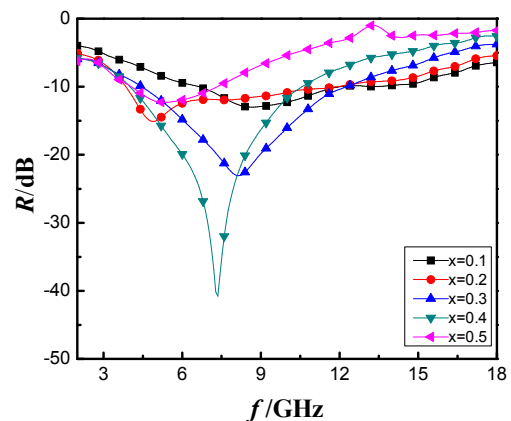


Figure 4. Variation of the reflection loss with frequency of $\text{Ba}(\text{MnZn})_x\text{Co}_{2(1-x)}\text{Fe}_{16}\text{O}_{27}$ ferrites at a thickness of 2.8 mm.

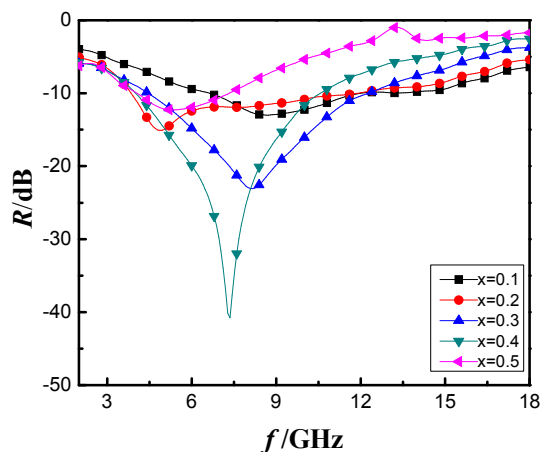


Figure 5. Variation of the reflection loss with frequency of $\text{Ba}(\text{MnZn})_{0.4}\text{Co}_{1.2}\text{Fe}_{16}\text{O}_{27}$ ferrites at different thicknesses.

-40.7 dB at a frequency of 7.3 GHz, with a bandwidth of 6.6 GHz for losses less than -10 dB. For $d = 3.2$ mm, the maximum reflection loss is approximately -32.5 dB at a frequency of 9.0 GHz, with a bandwidth 6.5 GHz for losses less than -10 dB. The absorption peak obviously exhibits a shift towards higher frequencies (blue shift) with an increase in the thickness of the samples. Thus, the matching thickness of $\text{Ba}(\text{MnZn})_{0.4}\text{Co}_{1.2}\text{Fe}_{16}\text{O}_{27}$ as a microwave absorber is 2.8 mm.

3.3. Electromagnetic Loss Mechanisms

Figure 6 shows the spectra of the complex permittivity and permeability of $\text{Ba}(\text{MnZn})_{0.4}\text{Co}_{1.2}\text{Fe}_{16}\text{O}_{27}$. The imaginary part ϵ'' of the permittivity is small, and the real part ϵ' is in the range of 5.5 - 6.5 over the frequency range of 2 - 18 GHz. The real part of the permeability decreases with an increase of frequency, but it does not change when the frequency exceeds 10 GHz. Two peaks of the imaginary part μ'' are located at 4.5 GHz and 8 GHz, but μ'' decreases when the frequency exceeds 4.5 GHz.

Using the dielectric loss tangent $\tan\delta_e = \epsilon''/\epsilon'$ and the magnetic loss tangent $\tan\delta_m = \mu''/\mu'$, the variation of $\tan\delta_e$ and $\tan\delta_m$ over the frequency range of 2 - 18 GHz can be determined. As shown in **Figure 7**, $\tan\delta_e$ is less than 0.1 and gradually changes with frequency over the entire frequency range, which indicates the presence of weak dielectric loss. This low loss may occur because doping will produce intrinsic electric dipole moments, thus forming defected dipoles. In the presence of a microwave electromagnetic field, polarization relaxation in the dipoles can lead to dielectric losses.

Relative to the dielectric loss $\tan\delta_e$, the magnetic loss $\tan\delta_m$ is much greater over the frequency range of 2 - 18 GHz. The value of $\tan\delta_m$ is greater than 0.3 over the frequency range of 2 - 15 GHz. There are two peaks on the

curve of $\tan\delta_m$, with the first peak exhibiting a value of 0.78 at approximately 4.5 GHz and the second peak exhibiting a value of 0.82 at approximately 8 GHz; these values are consistent with the peaks of μ'' shown in **Figure 6**. The peak position of the microwave reflectivity is predicted to be between the two magnetic loss tangent peaks, though closer to the second peak, which is consistent with the data shown in **Figure 4**.

The magnetic loss primarily results from domain wall displacement, domain turning, domain wall resonance and natural resonance. As shown in **Figure 7**, the first loss tangent peak originates from domain wall resonance, and the second peak originates from natural resonance, while magnetization relaxation is present over the entire frequency range. Doping with MnZn can result in the effect of domain wall pinning and the change of magnetic anisotropy, so the damping of domain turning and domain wall displacement increases, thus leading to resonance enhancement and resonance frequency-position shift. However, an excessive amount of doping may result in weak microwave absorption, due to the increase in electric resistivity from the enhancement of electron scattering and the increase of the lattice defects. Consequently, Ohmic loss is increased, and the microwave absorption is not conducive to impedance matching. As a result, a suitable amount of MnZn-doping is required to improve the microwave absorption of W-type barium-cobalt ferrites (as in **Figure 4**). In addition, because the powder morphology was hexagonal flaky, this shape anisotropy can result in magnetocrystalline anisotropy, which increases the microwave scattering in the medium, thereby enhancing the magnetic loss.

4. Conclusion

The crystal structure of MnZn-doped barium-cobalt ferrite $\text{Ba}(\text{MnZn})_x\text{Co}_{2(1-x)}\text{Fe}_{16}\text{O}_{27}$ ($x = 0.1, 0.2, 0.3, 0.4$ and 0.5) prepared using a sol-gel process was hexagonal W-type phase, and the samples exhibited a soft magnetism. Incorporating MnZn into the structure resulted in nearly no change in the structure with different doping amounts, and the morphology of the powders was hexagonal flaky with an average particle size of 5 μm . As a result, $\text{Ba}(\text{MnZn})_x\text{Co}_{2(1-x)}\text{Fe}_{16}\text{O}_{27}$ ferrite exhibits the excellent microwave absorption properties of wide bandwidth and strong loss over the frequency range of 2 - 18 GHz. The amount of MnZn doping will greatly influence the absorption properties of $\text{Ba}(\text{MnZn})_x\text{Co}_{2(1-x)}\text{Fe}_{16}\text{O}_{27}$. The reflection loss peak exhibited the characteristics of a maximum loss of -40.7 dB at a frequency of 7.3 GHz, with an effective bandwidth of 6.6 GHz for losses less than -10 dB when the thickness of the sample was 2.8 mm and $x = 0.4$. The microwave absorption of $\text{Ba}(\text{MnZn})_x\text{Co}_{2(1-x)}\text{Fe}_{16}\text{O}_{27}$ ferrite originated from weak

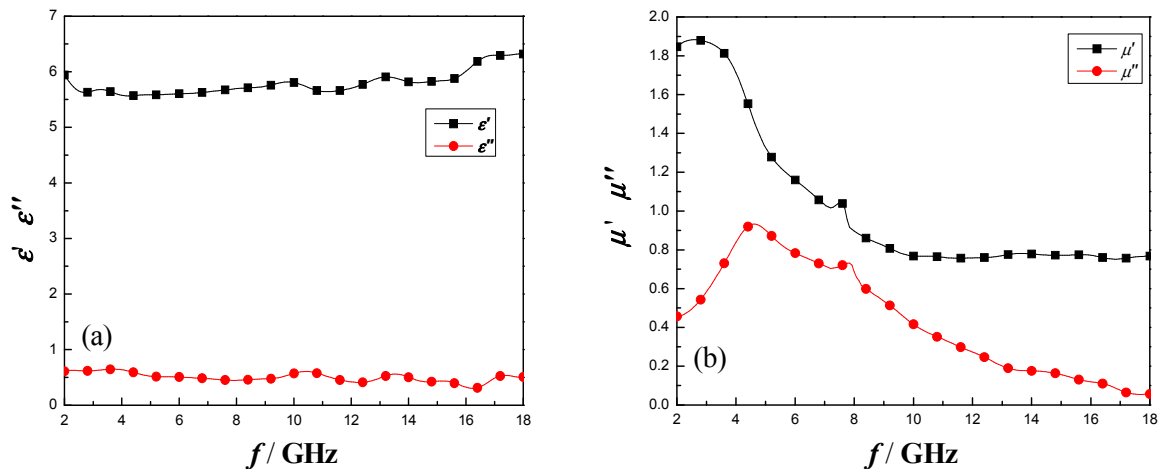


Figure 6. Spectra of the complex permittivity and permeability of $\text{Ba}(\text{MnZn})_{0.4}\text{Co}_{1.2}\text{Fe}_{16}\text{O}_{27}$. (a) permittivity: real part ϵ' and imaginary part ϵ'' ; (b) permeability: real part μ' and imaginary part μ'' .

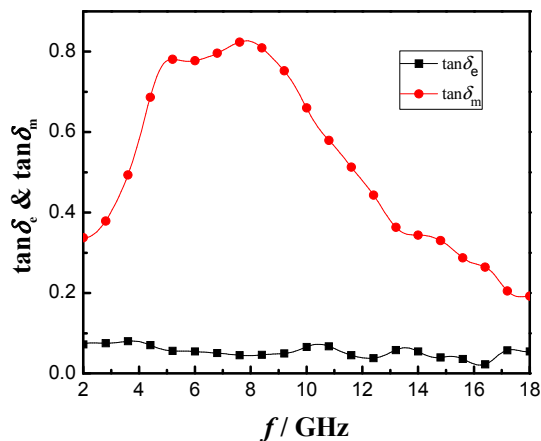


Figure 7. Variation of the dielectric loss $\tan\delta_e$ and the magnetic loss $\tan\delta_m$ with frequency for $\text{Ba}(\text{MnZn})_{0.4}\text{Co}_{1.2}\text{Fe}_{16}\text{O}_{27}$ ferrites.

dielectric loss and strong magnetic loss. The dielectric loss was caused by the polarization relaxation of dipoles, and the magnetic loss was caused by magnetization relaxation, domain wall and natural resonances. Both the suitable amount of doping of MnZn and the hexagonal flaky morphology of the powder particles are helpful for enhancing the electromagnetic loss of the ferrites.

REFERENCES

- [1] R. S. Meena, S. Bhattacharya and R. Chatterjee, "Complex Permittivity, Permeability and Microwave Absorbing Properties of $(\text{Mn}_{2-x}\text{Zn}_x)$ U-Type Hexaferrite," *Journal of Magnetism and Magnetic Materials*, Vol. 322, No. 19, 2010, pp. 2908-2914. [doi:10.1016/j.jmmm.2010.05.004](https://doi.org/10.1016/j.jmmm.2010.05.004)
- [2] A. Ghasemia, A. Hossienpourob, A. Morisako, A. Saatchi and M. Salehi, "Electromagnetic Properties and Microwave Absorbing Characteristics of Doped Barium Hexaferrite," *Journal of Magnetism and Magnetic Materials*, Vol. 302, No. 2, 2006, pp. 429-435. [doi:10.1016/j.jmmm.2005.10.006](https://doi.org/10.1016/j.jmmm.2005.10.006)
- [3] R. C. Pullar, "Hexagonal Ferrites: A Review of the Synthesis, Properties and Applications of Hexaferrite Ceramics," *Progress in Materials Science*, Vol. 57, No. 7, 2012, pp. 1191-1334. [doi:10.1016/j.pmatsci.2012.04.001](https://doi.org/10.1016/j.pmatsci.2012.04.001)
- [4] A. Ghasemi, A. Hossienpourob, A. Morisako and X. Liu, "Investigation of the Microwave Absorptive Behavior of Doped Barium Ferrites," *Materials & Design*, Vol. 29, No. 1, 2008, pp. 112-117. [doi:10.1016/j.matdes.2006.11.019](https://doi.org/10.1016/j.matdes.2006.11.019)
- [5] M. H. Shams, S. M. A. Salehi and A. Ghasemi, "Electromagnetic Wave Absorption Characteristics of Mg-Ti Substituted Ba-Hexaferrite," *Materials Letters*, Vol. 62, No. 10-11, 2008, pp. 1731-1733. [doi:10.1016/j.matlet.2007.09.073](https://doi.org/10.1016/j.matlet.2007.09.073)
- [6] S. Sugimoto, K. Haga, T. Kagotani and K. Inomata, "Microwave Absorption Properties of Ba M-Type Ferrite Prepared by a Modified Coprecipitation Method," *Journal of Magnetism and Magnetic Materials*, Vol. 290-291, 2005, pp. 1188-1191. [doi:10.1016/j.jmmm.2004.11.381](https://doi.org/10.1016/j.jmmm.2004.11.381)
- [7] A. Ghasemi, X. Liu and A. Morisako, "Magnetic and Microwave Absorption Properties of $\text{BaFe}_{12-x}(\text{Mn}_{0.5}\text{Cu}_{0.5}\text{Zr})_{x/2}\text{O}_{19}$ Synthesized by Sol-Gel Processing," *Journal of Magnetism and Magnetic Materials*, Vol. 316, No. 2, 2007, pp. e105-e108. [doi:10.1016/j.jmmm.2007.02.043](https://doi.org/10.1016/j.jmmm.2007.02.043)
- [8] S. Choopani, N. Keyhan, A. Ghasemi, A. Sharbati and R. Alam, "Structural, Magnetic and Microwave Absorption Characteristics of $\text{BaCo}_x\text{Mn}_x\text{Ti}_{2x}\text{Fe}_{12-4x}\text{O}_{19}$," *Materials Chemistry and Physics*, Vol. 113, No. 2-3, 2009, pp. 717-720. [doi:10.1016/j.matchemphys.2008.07.130](https://doi.org/10.1016/j.matchemphys.2008.07.130)
- [9] Y. Kim and S. Kim, "Magnetic and Microwave Absorbing Properties of Ti and Co Substituted M-Hexaferrites in Ka-Band Frequencies (26.5 - 40 GHz)," *Journal of Electroceramics*, Vol. 24, No. 4, 2010, pp. 314-318. [doi:10.1007/s10832-009-9575-x](https://doi.org/10.1007/s10832-009-9575-x)
- [10] M. Matsumoto and Y. Miyata, "A Gigahertz-Range Electromagnetic Wave Absorber with Wide Bandwidth Made

- of Hexagonal Ferrite,” *Journal of Applied Physics*, Vol. 79, No. 8, 1996, pp. 5486-5488. [doi:10.1063/1.362284](https://doi.org/10.1063/1.362284)
- [11] Z. F. Zi, J. M. Dai, Q. C. Liu, H. Y. Liu, X. B. Zhu and Y. P. Sun, “Magnetic and Microwave Absorption Properties of W-Type $\text{Ba}(\text{Zn}_x\text{Co}_{1-x})_2\text{Fe}_{16}\text{O}_{27}$ Hexaferrite Platelets,” *Journal of Applied Physics*, Vol. 109, No. 7, 2011, Article ID: 07E536-1-3.
- [12] M. R. Meshram, N. K. Agrawal, B. Sinha and P. S. Misra, “Characterization of M-Type Barium Hexagonal Ferrite-Based Wide Band Microwave Absorber,” *Journal of Magnetism and Magnetic Materials*, Vol. 271, No. 2-3, 2004, pp. 207-214. [doi:10.1016/j.jmmm.2003.09.045](https://doi.org/10.1016/j.jmmm.2003.09.045)
- [13] R. S. Meena, S. Bhattacharya and R. Chatterjee, “Complex Permittivity, Permeability and Microwave Absorbing Studies of $(\text{Co}_{2-x}\text{Mn}_x)$ U-Type Hexaferrite for X-Band (8.2 - 12.4 GHz) Frequencies,” *Materials Science and Engineering: B*, Vol. 171, No. 1-3, 2010, pp. 133-138. [doi:10.1016/j.mseb.2010.03.086](https://doi.org/10.1016/j.mseb.2010.03.086)
- [14] Y. Nie, H. H. He, Z. K. Feng, X. C. Zhang and X. M. Cheng, “Microwave Characterization of $(\text{Co}, \text{Zn})_2\text{W}$ Barium Hexagonal Ferrite Particles,” *Journal of Magnetism and Magnetic Materials*, Vol. 303, No. 2, 2006, pp. e423-e427.
- [15] F. Tabatabaie, M. H. Fathi, A. Saatchi and A. Ghasemi, “Microwave Absorption Properties of Mn- and Ti-Doped Strontium Hexaferrite,” *Journal of Alloys and Compounds*, Vol. 470, No. 1-2, 2009, pp. 332-335. [doi:10.1016/j.jallcom.2008.02.094](https://doi.org/10.1016/j.jallcom.2008.02.094)
- [16] S. Choopani, N. Keyhan, A. Ghasemi, A. Sharbathi, I. Maghsoudi and M. Eghbali, “Static and Dynamic Magnetic Characteristics of $\text{BaCo}_{0.5}\text{Mn}_{0.5}\text{Ti}_{1.0}\text{Fe}_{10}\text{O}_{19}$,” *Journal of Magnetism and Magnetic Materials*, Vol. 321, No. 13, 2009, pp. 1996-2000. [doi:10.1016/j.jmmm.2008.12.030](https://doi.org/10.1016/j.jmmm.2008.12.030)
- [17] S. P. Gairola, V. Verma, A. Singh, L. P. Purohit and R. K. Kotnala, “Modified Composition of Barium Ferrite to Act as a Microwave Absorber in X-Band Frequencies,” *Solid State Communications*, Vol. 150, No. 3-4, 2010, pp. 147-151. [doi:10.1016/j.ssc.2009.10.011](https://doi.org/10.1016/j.ssc.2009.10.011)
- [18] T. Kagotani, D. Fujiwara, S. Sugimoto, K. Inomata and M. Homma, “Enhancement of GHz Electromagnetic Wave Absorption Characteristics in Aligned M-Type Barium Ferrite $\text{Ba}_{1-x}\text{La}_x\text{Zn}_x\text{Fe}_{12-x-y}(\text{Me}_{0.5}\text{Mn}_{0.5})_y\text{O}_{19}$ ($x = 0.0 - 0.5$; $y = 1.0 - 3.0$; Me: Zr, Sn) by Metal Substitution,” *Journal of Magnetism and Magnetic Materials*, Vol. 272, 2004, pp. e1813-e1815.
- [19] X. Huang, J. Zhang, H. Wang, S. Yan, L. Wang and Q. Zhang, “ Er^{3+} -Substituted W-Type Barium Ferrite: Preparation and Electromagnetic Properties,” *Journal of Rare Earths*, Vol. 28, No. 6, 2010, pp. 940-943. [doi:10.1016/S1002-0721\(09\)60211-8](https://doi.org/10.1016/S1002-0721(09)60211-8)
- [20] A. Oikonomou, T. Giannakopoulou and G. Litsardakis, “Design, Fabrication and Characterization of Hexagonal Ferrite Multi-Layer Microwave Absorber,” *Journal of Magnetism and Magnetic Materials*, Vol. 316, No. 2, 2007, pp. e827-e830. [doi:10.1016/j.jmmm.2007.03.114](https://doi.org/10.1016/j.jmmm.2007.03.114)
- [21] P. Singh, V. K. Babbar, A. Razdan, R. K. Puri and T. C. Goel, “Complex Permittivity, Permeability, and x-Band Microwave Absorption of CaCoTi Ferrite Composites,” *Journal of Applied Physics*, Vol. 87, No. 9, 2000, pp. 4362-4365. [doi:10.1063/1.373079](https://doi.org/10.1063/1.373079)